Resurrecting the LHC discovery potential in the extended type-II seesaw model

Upalaparna Banerjee,[1,*] Christoph Englert,[2,†] and Wrishik Naskar[2,‡]

[1]*Indian Institute of Technology Kanpur, Kalyanpur, Kanpur 208016, Uttar Pradesh, India*
[2]*School of Physics & Astronomy, University of Glasgow, Glasgow G12 8QQ, United Kingdom*

(Received 8 April 2024; accepted 31 July 2024; published 4 September 2024)

The juxtaposition of the precision of lepton flavor measurements and the limited energy range of the Large Hadron Collider (LHC) to discover dynamical degrees of freedom linked to the generation of the observed lepton mass patterns naively suggests only a limited relevance of the LHC's high luminosity phase. This, potentially, extends to future colliders. Using the concrete example of the type-II seesaw model and its effective field theory extension, we show that blind directions create a rich phenomenological interplay of muon precision measurements and electroweak resonance searches at present and future colliders, with testable implications for the HL-LHC phase.

DOI: 10.1103/PhysRevD.110.055010

I. INTRODUCTION

The observed mass hierarchies in the lepton sector of the Standard Model (SM) of particle physics present a motivated source for physics beyond the SM. The history of, e.g., dynamically explaining the smallness of neutrino masses [1–4] is as illustrious as it is long. What singles out the neutrinos in comparison to the charged leptons is the plethora of model-building avenues that present themselves to generate mass terms. These can rely on the direct inclusion of right-handed neutrino SM singlets [5,6], on extending the scalar sector of the SM [7–12], or on employing direct couplings to matter to source mass terms via loop-effects [13,14]. Given that the neutrinos are related to the charged sector via gauge-invariance of the SM, the precision measurements that can be performed in the charged lepton sector have a wider phenomenological relevance in these scenarios. In particular for models with extra scalars, the requirement of nontrivial electroweak quantum numbers makes these states excellent targets for exotics searches at colliders, e.g., through Drell-Yan-like production as discussed in [15,16] (see Refs. [17–20] for recent searches at the Large Hadron Collider, LHC). The charged scalars have a rich phenomenology and can also be probed through low-energy meson decays, through off-shell production [21,22].

It is conceivable that mass scale of the degrees that underpin the generation of neutrino masses lies outside the direct sensitivity range of the LHC. While entirely possible, and even expected in, e.g., type-II seesaw mechanism scenarios, the relevant energy scales could even lie beyond the reach of future machines. However, if the new physics scenario does indeed deviate from its simplest implementation, new phenomenological implications can change this picture. In the context of seesaw mechanisms, in particular the precision measurements of $\mu \to 3e$ and $\mu \to e\gamma$ provide tight constraints that quickly push the mass scale of the new BSM degrees of freedom outside the LHC discovery potential.

In this work, to explore a related but different avenue, we consider modifications of the type-II seesaw model by including higher dimensional effective operators. Identifying a relevant set of couplings, we show that consistency with precision electroweak and muon data could still be compatible with resonances in the LHC-accessible energy regime. This comes at the price of a TeV-scale departure from the standard type-II scenario, which provides a testable implication in its own right. This work is organized as follows. In Sec. II A we swiftly introduce the type-II seesaw scenario to make this work self-contained. We then consider constraints on this model class in Sec. II B. In Sec. II C, we review these findings from the vantage point of nonminimal, TeV-scale modifications. These can move mass scales to a range that is probable at present and future colliders. We comment on the connection of the low-energy precision observables (we focus on muon physics) and its TeV scale implications via the renormalization group flow in Sec. II C 2 before concluding in Sec. III.

*Contact author: upalab@iitk.ac.in
†Contact author: christoph.englert@glasgow.ac.uk
‡Contact author: w.naskar.1@research.gla.ac.uk

II. PHENOMENOLOGY OF THE (DEFORMED) TYPE-II SEESAW MODEL

A. The model

The type-II seesaw offers a natural and a minimal framework to account for the smallness of observed neutrino masses, which comes about by extending the SM scalar sector minimally by an $\mathrm{SU}(2)_L$ triplet scalar Δ, characterized by a hypercharge $Y_\Delta = 1$. The inclusion of Δ leads to new terms in the scalar potential $V(\Phi, \Delta)$,

$$\begin{aligned} V(\Phi,\Delta) = &-m_H^2(\Phi^\dagger\Phi) + \lambda_H(\Phi^\dagger\Phi)^2 + m_\Delta^2\mathrm{Tr}[\Delta^\dagger\Delta] \\ &+ \lambda_{\Delta_1}(\mathrm{Tr}[\Delta^\dagger\Delta])^2 + \lambda_{\Delta_2}\mathrm{Tr}[(\Delta^\dagger\Delta)^2] \\ &+ \lambda_{\Delta_3}(\Phi^\dagger\Phi)\mathrm{Tr}[\Delta^\dagger\Delta] + \lambda_{\Delta_4}\Phi^\dagger\Delta\Delta^\dagger\Phi \\ &+ [\mu_\Delta\Phi^\dagger i\sigma^2\Delta^\dagger\Phi + \mathrm{H.c.}], \end{aligned} \tag{2.1}$$

where Φ denotes the original SM $\mathrm{SU}(2)_L$ doublet scalar. In addition to the neutral components, Δ also comprises singly-charged and doubly-charged scalars, holding significant phenomenological implications as direct probes of the type-II seesaw mechanism and its characteristics in various collider experiments [18,23–30]. We can explicitly express Φ and Δ in the following manner by expanding around their vacuum expectation values (vevs) denoted by v_Φ and v_Δ, respectively,

$$\begin{aligned} \Phi &= \frac{1}{\sqrt{2}}\begin{pmatrix} \sqrt{2}\phi^+ \\ (\phi + v_\Phi + i\eta) \end{pmatrix}, \\ \Delta &= \frac{1}{\sqrt{2}}\begin{pmatrix} \delta^+ & \sqrt{2}\Delta^{++} \\ (\delta^0 + v_\Delta + i\chi) & -\delta^+ \end{pmatrix}. \end{aligned} \tag{2.2}$$

Most importantly, the addition of the complex triplet results in novel Yukawa interactions between Δ and the left-handed lepton doublet (ψ_L). These are quintessential for generating nonzero neutrino masses through the nonzero vev of the complex triplet Δ after electroweak symmetry breaking (EWSB),

$$\mathcal{L}^{\mathrm{BSM}}_{\mathrm{Yukawa}} = -(Y_\Delta)_{ij}\bar{\psi}^c_{L_i}\Delta\psi_{L_j} + \mathrm{H.c.} \tag{2.3}$$

Here, Y_Δ is the BSM Yukawa coupling matrix. The Lagrangian for the type-II seesaw mechanism is therefore given by,

$$\mathcal{L}^{\text{type-II}} = \mathcal{L}_{\mathrm{SM}} + \mathrm{Tr}[D_\mu\Delta^\dagger D^\mu\Delta] - V(\Phi,\Delta) + \mathcal{L}^{\mathrm{BSM}}_{\mathrm{Yukawa}}. \tag{2.4}$$

After EWSB, the two vevs v_Φ and v_Δ contribute to the masses of the gauge bosons, with,

$$M_{W^\pm}^2 = \frac{g^2}{4}(v_\Phi^2 + 2v_\Delta^2), \quad M_Z^2 = \frac{g^2+g'^2}{4}(v_\Phi^2 + 4v_\Delta^2), \tag{2.5}$$

where g and g' are the coupling constants for the $SU(2)_L$ and $U(1)_Y$ gauge groups, respectively. The masses of the scalars become,

$$M^2_{\text{neutral, }CP\text{-even}} = \begin{pmatrix} 2\lambda_H v_\Phi^2 & -\sqrt{2}\mu_\Delta v_\Phi + v_\Delta v_\Phi(\lambda_{\Delta_3}+\lambda_{\Delta_4}) \\ -\sqrt{2}\mu_\Delta v_\Phi + v_\Delta v_\Phi(\lambda_{\Delta_3}+\lambda_{\Delta_4}) & \frac{\mu_\Delta v_\Phi^2}{\sqrt{2}v_\Delta} + 2v_\Delta^2(\lambda_{\Delta_1}+\lambda_{\Delta_2}) \end{pmatrix}, \tag{2.6}$$

$$M^2_{\text{neutral, }CP\text{-odd}} = \begin{pmatrix} 2\sqrt{2}\mu_\Delta v_\Delta & -\sqrt{2}\mu_\Delta v_\Phi \\ -\sqrt{2}\mu_\Delta v_\Phi & \frac{\mu_\Delta v_\Phi^2}{\sqrt{2}v_\Delta} \end{pmatrix}, \tag{2.7}$$

$$M^2_{\mathrm{charged}} = \begin{pmatrix} \frac{\mu_\Delta v_\Phi^2}{\sqrt{2}v_\Delta} - \frac{1}{4}v_\Phi^2\lambda_{\Delta_4} & -\mu_\Delta v_\Phi + \frac{v_\Phi v_\Delta \lambda_{\Delta_4}}{2\sqrt{2}} \\ -\mu_\Delta v_\Phi + \frac{v_\Phi v_\Delta\lambda_{\Delta_4}}{2\sqrt{2}} & \sqrt{2}\mu_\Delta v_\Delta - \frac{1}{2}v_\Delta^2\lambda_{\Delta_4} \end{pmatrix}, \tag{2.8}$$

$$M^2_{\Delta^{\pm\pm}} = \frac{\mu_\Delta v_\Phi^2}{\sqrt{2}v_\Delta} - v_\Delta^2\lambda_{\Delta_2} - \frac{1}{2}v_\Phi^2\lambda_{\Delta_4}. \tag{2.9}$$

Since Δ acquires nonzero vev, the scalar sector, apart from the doubly charged scalar ($\Delta^{\pm\pm}$) involves nontrivial mixing, as can be seen in Eqs. (2.6), (2.7), and (2.8). The physical states can be recovered in the following manner,

$$\begin{aligned} \begin{pmatrix} h \\ \Delta^0 \end{pmatrix} &= \begin{pmatrix} \cos\alpha & \sin\alpha \\ -\sin\alpha & \cos\alpha \end{pmatrix}\begin{pmatrix} \phi \\ \delta^0 \end{pmatrix}, \\ \begin{pmatrix} G^0 \\ A \end{pmatrix} &= \begin{pmatrix} \cos\beta_0 & \sin\beta_0 \\ -\sin\beta_0 & \cos\beta_0 \end{pmatrix}\begin{pmatrix} \eta \\ \chi \end{pmatrix}, \\ \begin{pmatrix} G^\pm \\ \Delta^\pm \end{pmatrix} &= \begin{pmatrix} \cos\beta_\pm & \sin\beta_\pm \\ -\sin\beta_\pm & \cos\beta_\pm \end{pmatrix}\begin{pmatrix} \phi^\pm \\ \delta^\pm \end{pmatrix}, \end{aligned} \tag{2.10}$$

with

$$\tan 2\alpha = \frac{v_\Phi[\sqrt{2}\mu_\Delta - v_\Delta(\lambda_{\Delta_3}+\lambda_{\Delta_4})]}{[v_\Phi^2(\frac{1}{2\sqrt{2}}\frac{\mu_\Delta}{v_\Delta}-\lambda_H)+v_\Delta^2(\lambda_{\Delta_1}+\lambda_{\Delta_2})]}, \quad (2.11)$$

$$\tan\beta_0 = 2v_\Delta/v_\Phi, \qquad \tan\beta_\pm = \sqrt{2}v_\Delta/v_\Phi. \quad (2.12)$$

In addition to the three Goldstone bosons (G^0 and $G^\pm$), this gives rise to additional singly-charged scalars $\Delta^\pm$, one CP-odd scalar A, and CP-even scalars Δ^0 and h. We identify the latter with the observed 125 GeV Higgs boson. By diagonalizing $M^2_{\text{neutral},CP\text{-even}}$, $M^2_{\text{neutral},CP\text{-odd}}$ and M^2_{charged}, we can determine the masses of the CP-even neutral scalars, CP-odd scalars and charged scalars respectively, while the masses of the Goldstone bosons are identically zero. The electroweak vev is defined as $v^2 \equiv v_\Phi^2 + 2v_\Delta^2 \approx (246\ \text{GeV})^2$, signalizing a violation of custodial isospin: the ratio of the gauge boson masses is parametrized by the ρ-parameter, given by $\rho = M_W^2/(M_Z^2\cos^2\theta_W)$, and the current electroweak precision constraints on ρ, sets an upper limit on the triplet vev $v_\Delta < 4.8$ GeV [24,27] at 95% CL. Upon EWSB, the new physics contributions to the Yukawa interactions in the neutrino sector are given by,

$$\mathcal{L}^{\text{BSM}}_{\text{Yukawa}} \supset \frac{v_\Delta}{\sqrt{2}}[(Y_\Delta + Y_\Delta^T)_{ij}\bar{\nu}_i^c\nu_j], \quad (2.13)$$

where i, and j are flavor indices. The neutrino mass-mixing matrix (M_ν) originating from the Lagrangian is diagonalized by the unitary Pontecorvo-Maki-Nakagawa-Sakata (PMNS) matrix,

$$M_\nu = U^*_{\text{PMNS}} M_\nu^{\text{diag}} U^\dagger_{\text{PMNS}}, \quad (2.14)$$

where $M_\nu^{\text{diag}} = \text{diag}(m_{\nu_1}, m_{\nu_2}, m_{\nu_3})$. The different m_{ν_i} represent the three physical neutrino masses; the Yukawa matrix therefore is given by,

$$Y_\Delta = \frac{M_\nu}{\sqrt{2}v_\Delta}. \quad (2.15)$$

The nature of the Yukawa matrix is thus determined by neutrino oscillation parameters and v_Δ. Non-zero neutrino mass-splittings allow for nonzero flavor off-diagonal couplings, which can lead to interesting lepton flavor violating signatures [31–33], which we further discuss in Sec. II B 3.

B. Constraints

The addition of the complex $SU(2)_L$ triplet gives rise to a large range of theoretical and phenomenological implications. The addition of several physical BSM scalars offer unique collider signatures, precision constraints, and novel interactions sensitive to various low-energy processes and unique decay channels. All of these approaches are effective in probing and constraining parts of the viable parameter space of the model. Constraints on this vast parameter space have been analyzed in the existing type-II seesaw literature. In particular, Ref. [24] has provided combined theoretical constraints from vacuum stability, perturbative unitarity, electroweak precision and Higgs boson data in terms of the triplet mass splittings ($\Delta M = M_{\Delta^\pm} - M_{\Delta^{\pm\pm}}$) and $M_{\Delta^{\pm\pm}}$ recently, with implications for the LHC. With the LHC Run-3 in progress, its high-luminosity phase on the horizon, and future facilities such as the FCC under active discussion [34–37], our analysis focuses on obtaining an updated status on the collider bounds, taking into account recent measurements performed by the ATLAS and CMS experiments [17–20] as reference points. Furthermore, we also comment on potentially improved future electroweak precision constraints and explore novel lepton flavor-violating processes predicted by the type-II seesaw model, which will be measured with higher precision soon.

1. Direct collider constraints

First, we are going to focus on constraining the parameter space of the type-II seesaw model using the wealth of collider analyses. In particular, we focus on the production of the doubly charged scalar ($\Delta^{\pm\pm}$) which is the primary LHC search channel and the smoking gun signal for the type-II seesaw mechanism. The main processes of interest are the pair production of these doubly charged scalars through the neutral-current Drell-Yan (DY)-like process mediated by virtual Z/γ contribution. Another relevant mode of production is via the charged-current interactions mediated by W bosons (see Fig. 1). The decay channels of interest for $\Delta^{\pm\pm}$ for these searches are mainly the decays into same-sign lepton pairs ($\Delta^{\pm\pm} \to l_\alpha^\pm l_\beta^\pm$ with $l = e, \mu$), and the decays into gauge bosons ($\Delta^{\pm\pm} \to W^\pm W^\pm$). In the limit of $v_\Delta \ll 0.1$ MeV($\ll v$), the dilepton channel dominates, and therefore, the four-lepton channel ($\Delta^{++}\Delta^{--} \to l^+l^+l^-l^-$) arising from the neutral-current DY process, will provide a clear BSM signature. This can be utilized to dramatically suppress expected backgrounds in the SM through sideband analyses of the same-sign mass spectra, which are experimentally under very good control (see [20,38–41]). The branching ratios related to the exclusive final states of the $\Delta^{\pm\pm}$ decay depends on the neutrino mass-mixing matrix and thus serve as a probe of its structure.

The ATLAS and CMS collaborations have been able to exclude masses of $\Delta^{\pm\pm}$ lighter than 850 GeV in their analyses, assuming a 100% decay into a light-lepton pair (ee, $\mu\mu$, or $e\mu$) [17,18]. From this, model-specific constraints can be obtained by direct rescaling of the branching ratios (which will also include tau contributions). For comparability, we will follow the discussion of [17,18]. For a larger v_Δ, however, the triplet Yukawa couplings

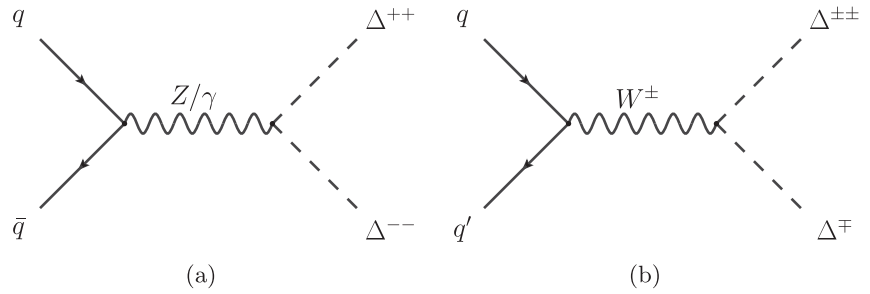

FIG. 1. Representative Feynman diagrams for the production of doubly charged scalars through (a) pair production via neutral-current DY and (b) associated production via charged-current DY processes.

become small, and the diboson decay channel dominates (at the price of rising tension with the ρ parameter). The limits set by ATLAS currently are at around 220 GeV for $v_\Delta = 0.1$ GeV [19], which is considerably weaker compared to the constraints from the dilepton channels.

The collider analyses carried out by ATLAS and CMS are not representative of the full parameter space of the model. They probe specific regions of the triplet vev (in particular, to the very low and very high values of v_Δ for the two decay channels), while assuming mass degeneracy of the scalar triplet masses. These assumptions render the decays of $\Delta^{\pm\pm}$ into same-sign leptons and dibosons phenomenologically dominant. Focussing on the experimentally and theoretically well-motivated four-lepton final states, we will estimate and compare the expected direct future bounds from the HL-LHC phase as well as a future hadron-hadron machine, extrapolating from the current analyses under identical assumptions.

To this end, we employ FEYNRULES [42] to create a model with normal neutrino mass hierarchy (i.e., $m_{\nu_1} < m_{\nu_2} < m_{\nu_3}$), which is interfaced with MADGRAPH_AMC@NLO [43] through the UFO package [44,45]. Events are generated at center-of-mass energies of $\sqrt{s} = 14$ TeV and $\sqrt{s} = 100$ TeV for the neutral current DY process: $pp \to \Delta^{++}\Delta^{--} \to l^+l^+l^-l^-$. This analysis assumes a 100% branching ratio. Our investigation is centred around the search for doubly charged scalars [16,18] with parton-level cuts to provide qualitative sensitivities at present and future colliders. We impose specific cuts, requiring all leptons ($l = e/\mu$) to be within the central part of the detector ($|\eta(l)| < 2.5$) and with a transverse momentum $p_T > 30$ GeV. Only leptons with no jet activity within the cone radius are considered ($\Delta R(j, l) < 0.4$), and the final states must contain exactly one positively-charged and one negatively-charged lepton pair; otherwise, the event is vetoed. An invariant mass cut is always applied for each lepton pair $M_{l^\pm l^\pm} > 200$ GeV.

Given that we expect the same-signed leptons to result from $\Delta^{\pm\pm}$ decays, we ensure the consistency of the two masses by calculating,

$$\bar{M} = \frac{M_{l^+l^+} + M_{l^-l^-}}{2}, \tag{2.16}$$

$$\Delta M = |M_{l^+l^+} - M_{l^-l^-}|. \tag{2.17}$$

The two masses are considered consistent if $\Delta M/\bar{M} < 0.25$, thus imposing a resonant signal character. Additionally, an event is vetoed if there exists an opposite-signed same-flavor lepton pair with an invariant mass in the range $M_{l^+l^-} \in [81.2, 101.2]$ GeV to suppress background resulting from Z decays.

The total number of signal events is then determined as $N_S = \sigma \times \mathcal{L} \times A$, where A represents acceptance. Assuming a good background subtraction which is possible through sideband analyses [20,38–40,46], we calculate the statistical significance at integrated luminosities $\mathcal{L} =$ 139 fb^{-1} and 3 ab^{-1} at $\sqrt{s} = 14$ TeV, obtaining 3σ mass sensitivities at the LHC and the high-luminosity limit, as depicted in Fig. 2(a). We calibrate our acceptance to reproduce the 3σ LHC bounds from the ATLAS search for doubly charged scalars reported in [18]. The expected 95% confidence limits (CL) shown by the blue dotted line in Fig. 2(a) is taken from [18] which demonstrates very good agreement as the reference point for our extrapolation. These mass limits also align with those reported in [18,30]. Applying the same methodology to $\sqrt{s} = 100$ TeV, we provide a rough estimate of the mass sensitivity at the FCC-hh with an integrated luminosity of $\mathcal{L} = 30$ ab^{-1}, as illustrated in Fig. 2(b). As usual in searches at low backgrounds, the sensitivity gain when moving to 100 TeV entirely stems from the much larger relevant partonic energy range that can be obtained. The scaling of sensitivities therefore directly reflects the available center-of-mass energy.

2. Electroweak precision constraints

To constrain the model parameter space indirectly (e.g., at a future lepton machine), we focus on constraints from electroweak precision observables, namely the S, T, and U oblique parameters. Following [47], we can obtain the oblique parameters as,

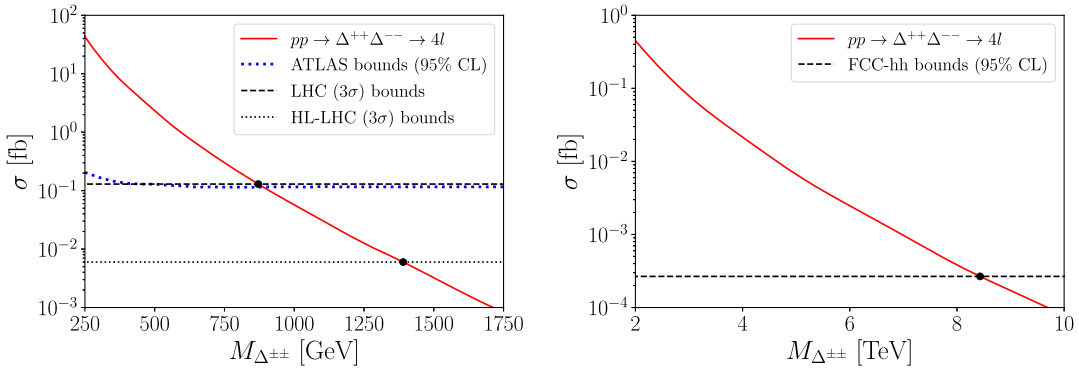

FIG. 2. Cross section for pair production of the doubly-charged scalars through neutral DY currents for (a) $\sqrt{s} = 14$ TeV and (b) $\sqrt{s} = 100$ TeV in the four-lepton final state (assuming a 100% branching ratio as Ref. [18,25]). The 3σ LHC (139 fb^{-1}) and HL-LHC (3 ab^{-1}) exclusion bounds are shown by the black dashed and dotted lines respectively on subfigure (a). The 95% CL on the search for $\Delta^{\pm\pm}$ with a 100% branching ratio into light leptons, cf. Ref. [18], is represented by the blue dotted line, showing a good agreement of our analysis. The 95% confidence bound for FCC-hh (30 ab^{-1}) is shown by the black dashed line on subfigure (b). These plots show that the LHC is sensitive to doubly charged scalars up to masses ∼870 GeV currently, and up to masses ∼1390 GeV in its high-luminosity phase. The FCC-hh will be sensitive to similar final states up to a mass scale of ∼8.5 TeV.

$$S = -\frac{1}{3\pi}\ln\frac{M^2_{\Delta^{\pm\pm}}}{M^2_{\Delta^0}} - \frac{2}{\pi}\left[(1-2s_W^2)^2\xi\left(\frac{M^2_{\Delta^{\pm\pm}}}{M_Z^2},\frac{M^2_{\Delta^{\pm\pm}}}{M_Z^2}\right) + s_W^4\xi\left(\frac{M^2_{\Delta^{\pm}}}{M_Z^2},\frac{M^2_{\Delta^{\pm}}}{M_Z^2}\right) + \xi\left(\frac{M^2_{\Delta^0}}{M_Z^2},\frac{M^2_{\Delta^0}}{M_Z^2}\right)\right], \tag{2.18a}$$

$$T = \frac{1}{8\pi c_W^2 s_W^2}\left[\eta\left(\frac{M^2_{\Delta^{\pm\pm}}}{M_Z^2},\frac{M^2_{\Delta^{\pm}}}{M_Z^2}\right) + \eta\left(\frac{M^2_{\Delta^{\pm\pm}}}{M_Z^2},\frac{M^2_{\Delta^{\pm}}}{M_Z^2}\right)\right], \tag{2.18b}$$

$$\begin{aligned} U = {} & \frac{1}{6\pi}\ln\frac{M^4_{\Delta^{\pm}}}{M^2_{\Delta^{\pm\pm}}M^2_{\Delta^0}} + \frac{2}{\pi}\left[(1-2s_W^2)^2\xi\left(\frac{M^2_{\Delta^{\pm\pm}}}{M_Z^2},\frac{M^2_{\Delta^{\pm\pm}}}{M_Z^2}\right) + s_W^4\xi\left(\frac{M^2_{\Delta^{\pm}}}{M_Z^2},\frac{M^2_{\Delta^{\pm}}}{M_Z^2}\right) + \xi\left(\frac{M^2_{\Delta^0}}{M_Z^2},\frac{M^2_{\Delta^0}}{M_Z^2}\right)\right] \\ & - \frac{2}{\pi}\left[\xi\left(\frac{M^2_{\Delta^{\pm\pm}}}{M_W^2},\frac{M^2_{\Delta^{\pm}}}{M_W^2}\right) + \xi\left(\frac{M^2_{\Delta^{\pm\pm}}}{M_W^2},\frac{M^2_{\Delta^{\pm}}}{M_W^2}\right)\right], \end{aligned} \tag{2.18c}$$

where the functions ξ and η are defined as,

$$\begin{aligned} \xi(x,y) &= \frac{4}{9} - \frac{5}{12}(x+y) + \frac{1}{6}(x-y)^2 + \frac{1}{4}\left[x^2 - y^2 - \frac{1}{3}(x-y)^3 - \frac{x^2+y^2}{x-y}\right]\ln\frac{x}{y} - \frac{1}{12}d(x,y)f(x,y), \\ \eta(x,y) &= x + y - \frac{2xy}{x-y}\ln\frac{x}{y}, \\ d(x,y) &= -1 + 2(x+y) - (x-y)^2, \\ f(x,y) &= \begin{cases} -2\sqrt{d(x,y)}\left[\arctan\dfrac{x-y+1}{\sqrt{d(x,y)}} - \arctan\dfrac{x-y-1}{\sqrt{d(x,y)}}\right], & d(x,y) > 0 \\ \sqrt{-d(x,y)}\ln\dfrac{x+y-1+\sqrt{-d(x,y)}}{x+y-1-\sqrt{-d(x,y)}}, & d(x,y) \le 0 \end{cases}. \end{aligned} \tag{2.18d}$$

Assuming degeneracy of the triplet masses ($M_{\Delta^0} \simeq M_{\Delta^\pm} \simeq M_{\Delta^{\pm\pm}}$), constraints reported by the GFITTER collaboration [48] impose $M_{\Delta^{\pm\pm}} \gtrsim 35$ GeV at 95% CL. To get an estimate on the constraints in future from electroweak precision observables [49,50], motivated from TLEP [51] and GigaZ [52], we reduce the uncertainties in S, T, and U obtained from GFITTER by an order of magnitude, and we obtain a limit on $M_{\Delta^{\pm\pm}} \gtrsim 105$ GeV at 95% CL. This implies that even dramatically improved electroweak precision measurements of oblique parameters at future lepton colliders (such as FCC-ee) will not lead to significant sensitivity enhancements. Nonoblique vertex corrections,

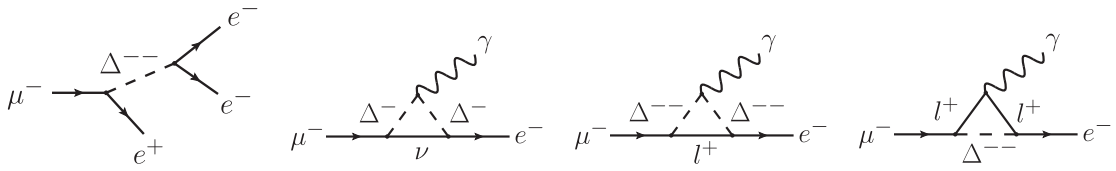

FIG. 3. Representative Feynman diagrams for the lepton flavor violating decays $\mu \to 3e$ and $\mu \to e\gamma$.

on the other hand, might provide a complementary avenue to probe nontrivial flavor structures in case such high precision related to the electroweak input parameter set of the SM is achieved.

3. Constraints from lepton flavor violating decays

The Yukawa interactions presented in Eq. (2.3), naturally lead to flavor-changing lepton decays such as $l_i^- \to l_j^+ l_k^- l_l^+$ and $l_i^- \to l_j^- \gamma$ [31,53–55]. In this work, we are specifically interested in two such lepton flavor violating decays, $\mu \to 3e$ and $\mu \to e\gamma$ (see Fig. 3). The former arises at tree-level, mediated by the doubly charged scalar ($\Delta^{\pm\pm}$), and its branching ratio is given by,

$$\mathrm{BR}(\mu \to 3e) = \frac{|(Y_\Delta)_{ee}(Y_\Delta)^*_{\mu e}|^2}{4G_F^2 M^4_{\Delta^{\pm\pm}}}, \tag{2.19}$$

where $G_F \simeq 1.166 \times 10^{-5}\ \mathrm{GeV}^{-2}$ is the Fermi constant. Setting $v_\Delta = 1$ eV, and $m_{\nu_1} = 0.05$ eV, and using the global fit of neutrino oscillations data from NuFIT [56], sets a lower limit on $M_{\Delta^{\pm\pm}} \gtrsim 1650$ GeV, from the current $\mathrm{BR}(\mu \to 3e) < 10^{-12}$ constraint [57], which is well beyond the reach of the current LHC sensitivity regime, as shown in Fig. 2. $\mu \to e\gamma$ occurs through one-loop penguin diagrams, mediated by $\Delta^\pm$ or $\Delta^{\pm\pm}$. In the process mediated by $\Delta^\pm$, the photon is emitted exclusively from the $\Delta^\pm$ boson at one-loop, whereas for the $\Delta^{\pm\pm}$ contribution, the photon can be emitted from either $\Delta^{\pm\pm}$ or the charged fermion propagator in the loop. The contributions from both scalars interfere coherently as they couple to leptons with the same chirality, resulting in a branching fraction [24],

$$\mathrm{BR}(\mu \to e\gamma) = \frac{\alpha_{\mathrm{EM}}}{192\pi G_F^2} |Y_\Delta^\dagger Y_\Delta|^2_{\mu e} \left(\frac{1}{M^2_{\Delta^\pm}} + \frac{8}{M^2_{\Delta^{\pm\pm}}} \right)^2, \tag{2.20}$$

with the electromagnetic fine-structure constant $\alpha_{\mathrm{EM}} \simeq 1/137$.

Setting $v_\Delta = 1$ eV, $M_{\Delta^\pm} \sim M_{\Delta^{\pm\pm}}$, and $m_{\nu_1} = 0.05$ eV we obtain $M_{\Delta^{\pm\pm}} \gtrsim 850$ GeV, from the current $\mathrm{BR}(\mu \to e\gamma) < 3.1 \times 10^{-13}$ constraint [58,59]. Assuming degeneracy in the masses of the charged triplet scalars, and using the neutrino oscillation data from NuFIT, both the branching ratios contain three free parameters, v_Δ, m_{ν_1} and $M_{\Delta^{\pm\pm}}$. The current limits on both these branching ratios can be used to obtain constraints on the resulting parameter space as illustrated in Fig. 4, where the shaded regions show the parts of the parameter space currently excluded by these constraints. The plots indicate that the regions not excluded by the lepton flavor violating constraints lie mostly beyond the reach of current LHC sensitivity, as well as the HL-LHC, especially for the $\mu \to 3e$ process. More precise measurements for these decays are going to push the mass limit even further beyond the reach of colliders. Any potential discovery at the LHC that phenomenologically fits the experimentally clean $\Delta^{\pm\pm}$ expectation could therefore point toward a richer phenomenology

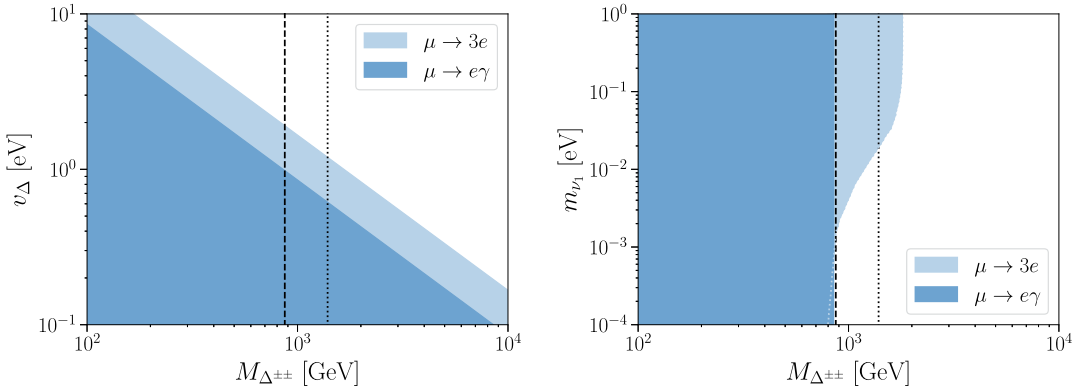

FIG. 4. Constraints from $\mu \to 3e$ and $\mu \to e\gamma$ for (a) $m_{\nu_1} = 0.05$ eV, and (b) $v_\Delta = 1$ eV. The black dashed and dotted lines on both plots represent the 3σ LHC and HL-LHC exclusion limits, respectively.

of the TeV scale than predicted by the vanilla type-II seesaw model. We turn to this in the next section.

C. Implications of EFT deformations

In this section, we extend the parameter space of the type-II seesaw model with EFT deformations to analyse the implications of a reduced $\Delta^{\pm\pm}$ mass scale within the LHC's sensitivity reach. This provides a new perspective for accommodating or predicting TeV-scale resonances in the light of highly constraining lepton flavor experiments. To this end, we construct the gauge-invariant dimension-6 structures that incorporate at least one Δ in addition to the usual dimension-6 SMEFT interactions [60] and analyse their implications. This construction, which we refer to as a "BSM-EFT" scenario, is justified by the possibility that the least massive non-SM particle might exist not very far from the electroweak scale, making it accessible to upcoming collider experiments, including improved analysis techniques for the HL-LHC phase [61].

The potential discovery of charged scalars in future colliders has been extensively studied in the literature within various BSM models, e.g., complex singlets [62–66], the two-Higgs doublet model (2HDM) [67–71], or complex-triplet extensions [16,72–75]. This further motivates the idea of extending these scenarios with EFT interactions to obtain a qualitative understanding of energy scales beyond the reach of current colliders. In parallel, these interactions highlight correlation constraints that are theoretically imposed by the most direct implementation of a certain model.[1] The gauge-invariant structures of the relevant operators have been adopted from Refs. [60,77].

Given that the constraints from $\mu \to 3e$ set the mass scale well beyond the reach of the LHC sensitive regime as discussed in Sec. II B 3, we focus on the impact of EFT deformations on this particular lepton flavor violating process in our analysis. The gauge-invariant dimension-6 operators for the SM extended by a complex triplet scalar, relevant for $\mu \to 3e$ have been tabulated in Table I. We trace their phenomenological relevance again by using FEYNRULES. We use FEYNARTS [78], and FORMCALC [79] for the analytical computation of the $\mu \to 3e$ branching ratio including the EFT extensions.

We first look at whether the dimension-6 modifications of the Yukawa couplings have an impact on the mass constraints from $\mu \to 3e$. The operators $\mathcal{O}^{(1)}_{L\Phi\Delta,ij}$, $\mathcal{O}^{(2)}_{L\Phi\Delta,ij}$, $\mathcal{O}^{(1)}_{L\Delta,ij}$, and $\mathcal{O}^{(2)}_{L\Delta,ij}$ lead to modifications of the Yukawa couplings for Δ after EWSB. The contributions from

TABLE I. Relevant dimension-6 operators for SM extended by a complex triplet scalar (Δ) [60,77,80], contributing to $\mu \to 3e$, where i, j, k, m are flavor indices, and α, β are SU(2) indices. Φ represents the SM Higgs doublet.

$\mathcal{O}^{(1)}_{L\Phi\Delta,ij}$	$(\bar{\psi}^c_{L_i}\Delta\psi_{L_j})(\Phi^\dagger\Phi)$	$\mathcal{O}^{(2)}_{L\Phi\Delta,ij}$	$\bar{\psi}^c_{L_i,\alpha}\Delta\Phi^\alpha\Phi^\dagger_\beta\psi^\beta_{L_j}$
$\mathcal{O}^{(1)}_{L\Delta,ij}$	$(\bar{\psi}^c_{L_i}\Delta\psi_{L_j})\mathrm{Tr}[(\Delta^\dagger\Delta)]$	$\mathcal{O}^{(2)}_{L\Delta,ij}$	$\bar{\psi}^c_{L_i}\Delta\Delta^\dagger\Delta\psi_{L_j}$
$\mathcal{O}^{ijkm}_{ll}$	$(\bar{\psi}_{L_i}\gamma_\mu\psi_{L_j})(\bar{\psi}_{L_k}\gamma^\mu\psi_{L_m})$	$\mathcal{O}^{ijkm}_{ee}$	$(\bar{e}_i\gamma_\mu e_j)(\bar{e}_k\gamma^\mu e_m)$
$\mathcal{O}^{ijkm}_{le}$	$(\bar{\psi}_{L_i}\gamma_\mu\psi_{L_j})(\bar{e}_k\gamma^\mu e_m)$	$\mathcal{O}^{ij}_{e\phi}$	$(\Phi^\dagger\Phi)(\bar{\psi}_{L_i}e_j\Phi)$

$\mathcal{O}^{(1)}_{L\Phi\Delta,ij}$ get absorbed into the Yukawa matrix Y_Δ while generating neutrino masses, and the contributions from $\mathcal{O}^{(1)}_{L\Delta,ij}$ and $\mathcal{O}^{(2)}_{L\Delta,ij}$ are suppressed by $v_\Delta^2 \ll v^2$ after EWSB. Therefore, the modified Yukawa couplings will have dominant contributions from $\mathcal{O}^{(2)}_{L\Phi\Delta,ij}$ in the parameter region that we have considered above. Upon EWSB, the modified Yukawa couplings (effectively modifying the mass-Yukawa coupling relation of the vanilla type-II seesaw model) can then be written as,

$$Y^{\text{mod.}}_{ij} = (Y_\Delta)_{ij} - \frac{C^{\text{BSM}}_{ij} v^2}{2\Lambda^2}, \tag{2.21}$$

where the C^{BSM}_{ij} is the Wilson coefficient corresponding to the effective operator $\mathcal{O}^{(2)}_{L\Phi\Delta,ij}$. Entering the modified Yukawa couplings into the $\text{BR}(\mu \to 3e)$ in Eq. (2.19), setting $v_\Delta = 1$ eV, $m_{\nu_1} = 0.05$ eV, and $M_{\Delta^{\pm\pm}} = 500$ GeV such that exotics searches imply a discovery at the LHC, we can constrain the Wilson coefficients to the region depicted in Fig. 5(a). Since the diagonal Yukawas are $\sim$2 orders of magnitude larger than the off-diagonal counterparts, Fig. 5(a) clearly illustrates that larger cancellations ($\sim$2 orders of magnitude) are required in the ee direction compared to μe. $\mu \to 3e$ also gets direct contributions from SMEFT 4-lepton operators ($\mathcal{O}^{ijkm}_{ll}$, $\mathcal{O}^{ijkm}_{ee}$, and $\mathcal{O}^{ijkm}_{le}$). The contributions from $\mathcal{O}^{ij}_{e\phi}$ however, are suppressed. We therefore do not include these in our analysis. Non-zero Wilson coefficients for the relevant SMEFT operators (in particular $\mathcal{O}^{1112}_{ll}$, $\mathcal{O}^{1112}_{ee}$, $\mathcal{O}^{1112}_{le}$, $\mathcal{O}^{1211}_{le}$) change the allowed parameter space for the Wilson coefficients of $\mathcal{O}^{(2)}_{L\Phi\Delta,ij}$, which can be seen from Fig. 5(b).

To check how far we can bring the mass scale down, we set $v_\Delta = 1$ eV, $m_{\nu_1} = 0.05$ eV and $C^{\text{BSM}}_{ee} = C^{\text{BSM}}_{\mu e}$. Since we obtain tighter constraints along μe compared to ee, the latter condition was assumed to obtain the tightest constraints on the BSM-EFT Wilson coefficients, assuming them to be of the same order of magnitude. From the $\mu \to 3e$ constraints, we obtain the plots shown in Fig. 6, which illustrates mass scales well within the region sensitive to the LHC are achievable while satisfying

[1]For instance, it is known that EFT deformations can significantly modify the phase transition history of the early universe physics, thereby accessing parameter regions that are seemingly excluded by LHC measurements of the 2HDM [69] with implications for the LHC exotics program [70]. Similar observations have been to reconcile the anomalous muonic $g-2$ with leading order constraints of Higgs sector extensions [16,76].

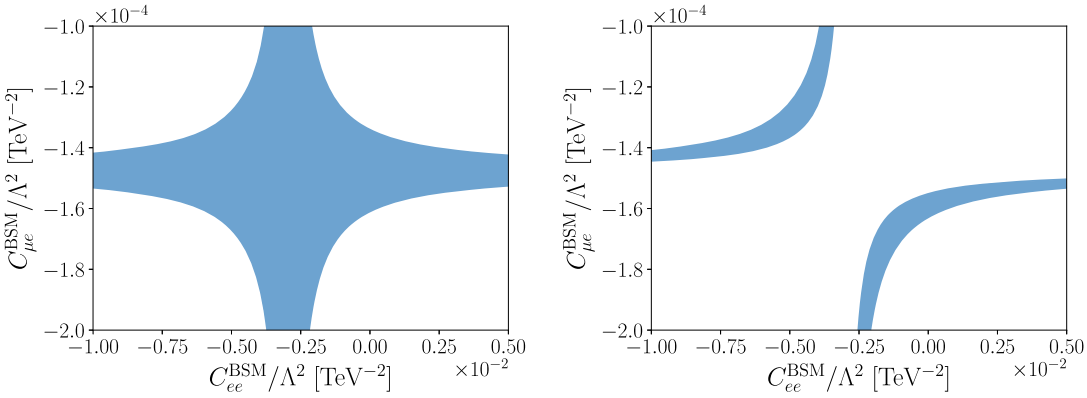

FIG. 5. Allowed regions from $\mu \to 3e$ on Wilson coefficients ($C_{\mu e}^{\rm BSM}$ and $C_{ee}^{\rm BSM}$) for $M_{\Delta^{\pm\pm}} = 500$ GeV (a) without contributions from the SMEFT 4-lepton operators, and (b) setting $C_{ll}^{1112}/\Lambda^2 = C_{le}^{1112}/\Lambda^2 = C_{le}^{1211}/\Lambda^2 = C_{ee}^{1112}/\Lambda^2 = 2.5 \times 10^{-6}$ TeV^{-2}.

constraints from $\mu \to 3e$. To present a complete argument on this front, we perform a similar analysis for $\mu \to e\gamma$. The modified Yukawas outlined in Eq. (2.21) directly contribute to the $\mu \to e\gamma$ branching ratio given in Eq. (2.20). Additionally, the SMEFT operators that contribute to $\mu \to e\gamma$ at tree-level [81] are listed in Table II. We illustrate our results to this front on Fig. 6 elucidating the fact that we can still probe mass scales within (HL-)LHC sensitivity. As anticipated, cancellations from the SMEFT operators fine-tune and tighten the constraints on the BSM-EFT Wilson coefficients.

The combined exclusion contours from $\mu \to 3e$ on the Wilson coefficients corresponding to the SMEFT 4-lepton operators and the relevant BSM-EFT operators are presented in Fig. 7, for three chosen benchmark mass scales, $M_{\Delta^{\pm\pm}} = 870$ GeV (representing the current LHC-exclusion limit), 1 TeV and 1.4 TeV (representing the projected HL-LHC exclusion limit). This plot further elucidates the decrease in the allowed parameter space as one tries to bring the mass scale down to the LHC observable region. The constraints on the SMEFT-parametrized Wilson coefficients that improve the tension between the $\Delta^{\pm\pm}$ states and low energy measurements are relatively weak, and further discrimination of the two directions would predominantly be driven by a direct resolution of the cutoff scale, e.g., at a future FCC-hh. It is worth noting that experiments like MUONE [82,83] are unlikely to provide additional constraints as they predominantly fingerprint the low Q^2 behavior of the scattering process, although the experiment should be sensitive to the signature of $\mu e \to ee$.

TABLE II. Relevant SMEFT dimension-6 operators [60], contributing to $\mu \to e\gamma$, where i, j are flavor indices, μ, ν are Lorentz indices, and α, β are SU(2) indices. Φ represents the SM Higgs doublet.

$\mathcal{O}_{eW}$	$(\bar{\psi}_{L_i}\sigma^{\mu\nu}e_j)\tau^\alpha\Phi W^\alpha_{\mu\nu}$	$\mathcal{O}_{eB}$	$(\bar{\psi}_{L_i}\sigma^{\mu\nu}e_j)\Phi B_{\mu\nu}$

1. TeV-modified seesaw at colliders

The SMEFT four-lepton operators contributing to $\mu \to 3e$ can be probed directly at electron-positron machines through the process $e^+e^- \to e^\pm\mu^\pm$. We generate events for this process on MADGRAPH_AMC@NLO with the UFO model updated with the relevant dimension-6 operators, for the FCC-ee running at the Z boson pole at 192 ab^{-1}, and calibrate our acceptance to reproduce the bounds on 4-lepton operators presented in Refs. [84,85]. The 2σ-bounds on these operators is $|C_{4f}^{\rm SMEFT}| \lesssim 10^{-4}$ TeV^{-2}. At a future ee-Collider with $\sqrt{s} = 3$ TeV, with an integrated luminosity of 5 ab^{-1} this improves to $|C_{4f}^{\rm SMEFT}| \lesssim 10^{-5}$ TeV^{-2} [84], therefore implying that $\mu \to 3e$ will set more stringent bounds on these Wilson coefficients than future ee-colliders.

In the context of hadron colliders, these effective operators do not play a role in the production processes of triplet scalars. The dimension-6 BSM-EFT operators that modify the Yukawa couplings do influence the branching ratios; however, given that we have assumed mass configurations with dominant branching ratios for the doubly charged scalar decaying into light-leptons (e, μ), this does not imply a sensitivity enhancement compared to our prior analysis. What is more relevant for the production of the doubly-charged scalars is the relevance of the potential EFT deformations to the $Z/\gamma - \Delta^{++} - \Delta^{--}$ vertex. This would induce modifications of the pair production cross sections.

In Table III, we collect the structures that lead to modifications of the $(Z/\gamma)\Delta^{++}\Delta^{--}$ interactions. It is worth noting that the contributions from these operators would lead to an enhanced (when including squared dimension-6 contributions) cross-section for the DY production of $\Delta^{\pm\pm}$, which in principle should provide updated and improved

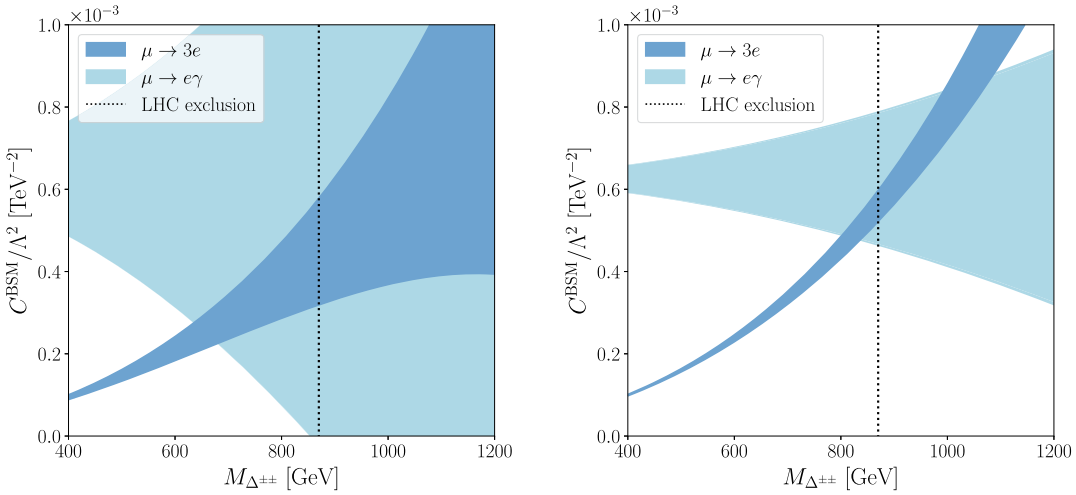

FIG. 6. The allowed parameter space of the BSM-EFT Wilson coefficients and $M_{\Delta^{\pm\pm}}$ for (a) $C_{ll}^{1112} = C_{le}^{1112} = C_{le}^{1211} = C_{ee}^{1112} = C_{4f}^{\rm SMEFT} = 0$, $C_{eB} = C_{eW} = C_{\mu\to e\gamma}^{\rm SMEFT} = 0$ and (b) $C_{4f}^{\rm SMEFT}/\Lambda^2 = 2.5 \times 10^{-6}$ TeV^{-2}, and $C_{\mu\to e\gamma}^{\rm SMEFT}/\Lambda^2 = 0.5 \times 10^{-6}$ TeV^{-2}. Here, $C_{ee}^{\rm BSM} = C_{\mu e}^{\rm BSM} = C^{\rm BSM}$. The black dotted lines on both plots represent the LHC exclusion limits.

limits on $M_{\Delta^{\pm\pm}}$ from collider analyses as functions of these Wilson coefficients. The analyses performed in the context of the renormalizable type-II scenario therefore provide conservative estimates of the sensitivity reach, predominantly making the mass scales of the type-II exotic states accessible to collider experiments. More precise measurements of the neutrino oscillation parameters from various experiments, along with updated measurements of the ρ-parameter providing a more accurate estimate of v_Δ, which essentially fixes the Yukawa matrix, would lead to a more precise determination of the hadron-collider sensitive region for the model. Similarly, we can expect analyses of the $\Delta^\pm$ states to add additional sensitivity, however, with reduced experimental sensitivity due to a significant amount of missing energy and a smaller electroweak coupling.

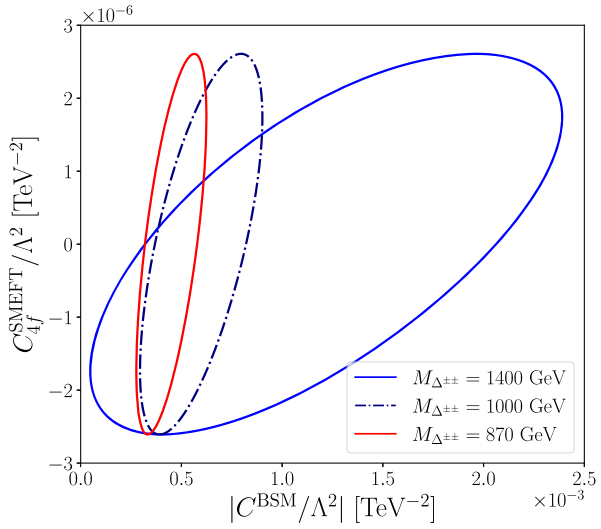

FIG. 7. Exclusion contours on SMEFT and BSM-EFT Wilson coefficients for $M_{\Delta^{\pm\pm}} = 870, 1000, 1400$ GeV from BR$(\mu \to 3e)$ limits, where $C_{ee}^{\rm BSM} = C_{\mu e}^{\rm BSM} = C^{\rm BSM}$, and $C_{ll}^{1112} = C_{le}^{1112} = C_{le}^{1211} = C_{ee}^{1112} = C_{4f}^{\rm SMEFT}$.

2. Impact of RGE running

As the μ experiments probe very different energy scales of the theory compared to the collider searches, RGE effects can *a priori* be important. Below the mass scales of the Higgs sector exotics (which we assume to be degenerate), the running of the SM couplings are unchanged. To estimate the relevance of these effects, e.g., at the scale of resonance ($M_\Delta \gg m_\mu$) we can map the modified Δ-contributions on the SMEFT four-fermion interaction that accurately describes $\mu \to 3e$ at the scale of the muon $m_\mu \ll M_\Delta$. The amplitude is then parametrized by,

$$C_{ll,\rm BSM}^{1112}(M_{\Delta^{\pm\pm}}^2) = C_{ll}^{1112}(M_{\Delta^{\pm\pm}}^2) - Y_{ee}^{\rm mod.}(Y_{\mu e}^{\rm mod.})^*, \qquad (2.22)$$

where $Y_{ij}^{\rm mod.}$ can be written in terms of BSM Yukawa couplings $(Y_\Delta)_{ij}$ and the BSM-EFT Wilson coefficients as shown in Eq. (2.21). We then compute the RGE flow of the SMEFT Wilson coefficients including the BSM effects, using DSIXTOOLS [86,87] and WILSON [88], between

TABLE III. Dimension-6 operators for SM extended by a complex triplet scalar (Δ) [60,77,80], relevant for Drell-Yan production of $\Delta^{\pm\pm}$.

$\mathcal{O}_{\Phi\Delta D}^{(1)}$	$[\Phi^\dagger(D_\mu\Delta)][(D^\mu\Delta)^\dagger\Phi]$	$\mathcal{O}_{\Phi\Delta D}^{(2)}$	$[\Delta^\dagger(D_\mu\Phi)][(D^\mu\Phi)^\dagger\Delta]$
$\mathcal{O}_{\Phi\Delta D}^{(3)}$	$\mathrm{Tr}[(\Delta^\dagger\Delta)][(D_\mu\Phi)^\dagger(D^\mu\Phi)]$	$\mathcal{O}_{\Phi\Delta D}^{(4)}$	$(\Phi^\dagger\Phi)\mathrm{Tr}[(D_\mu\Delta)^\dagger(D^\mu\Delta)]$

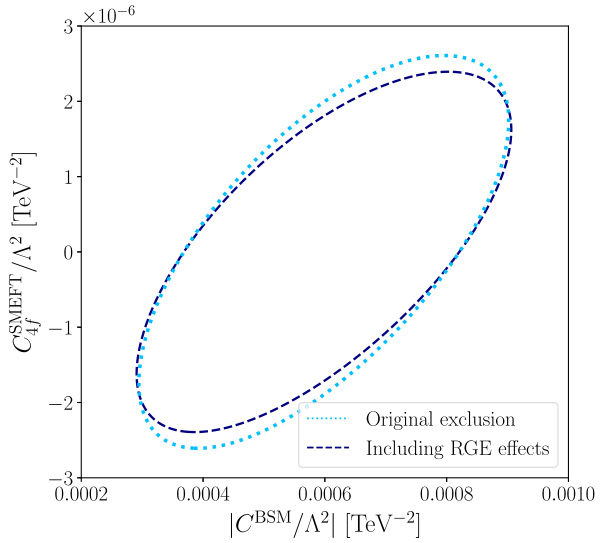

FIG. 8. Effect of RGE running on the allowed parameter space of SMEFT and BSM-EFT Wilson coefficients, corresponding to $\mu \to 3e$ constraints, for $M_{\Delta^{\pm\pm}} = 1000\,\mathrm{GeV}$. Here $C_{ee}^{\mathrm{BSM}} = C_{\mu e}^{\mathrm{BSM}} = C^{\mathrm{BSM}}$, and $C_{ll}^{1112} = C_{le}^{1112} = C_{le}^{1211} = C_{ee}^{1112} = C_{4f}^{\mathrm{SMEFT}}$.

$\Lambda_\mu = m_\mu = 105$ MeV and the scale of the resonance $\Lambda_{\mathrm{UV}} = M_\Delta$ to obtain a qualitative estimate of the impact of the renormalization group flow.

The RG evolution of the Wilson coefficients of the four-fermion operators from Λ_μ up to the scale of resonance $\Lambda_{\mathrm{UV}} = 1$ TeV is given by

$$C_{ll,\mathrm{BSM}}^{1112}(\Lambda_{\mathrm{UV}}) = 1.121 \times C_{ll}^{1112}(\Lambda_\mu) + 0.003 \times C_{le}^{1211}(\Lambda_\mu), \tag{2.23}$$

$$C_{ee}^{1112}(\Lambda_{\mathrm{UV}}) = 1.113 \times C_{ee}^{1112}(\Lambda_\mu) + 0.005 \times C_{le}^{1112}(\Lambda_\mu), \tag{2.24}$$

$$C_{le}^{1112}(\Lambda_{\mathrm{UV}}) = 0.963 \times C_{le}^{1112}(\Lambda_\mu) + 0.021 \times C_{ee}^{1112}(\Lambda_\mu), \tag{2.25}$$

$$C_{le}^{1211}(\Lambda_{\mathrm{UV}}) = 0.968 \times C_{le}^{1211}(\Lambda_\mu) + 0.003 \times C_{ll}^{1112}(\Lambda_\mu). \tag{2.26}$$

For this specific resonance scale ($M_\Delta = 1$ TeV), with $v_\Delta = 1$ eV and $m_{\nu_1} = 0.05$ eV for computing Yukawa couplings, as previously chosen, we substitute the expressions in Eqs. (2.23)–(2.26) for the SMEFT Wilson coefficients into the $\mu \to 3e$ branching ratio. The resulting exclusions on the parameter space of the Wilson coefficients of the relevant SMEFT and BSM-EFT operators are depicted in Fig. 8. We conclude that the RGE flow does not qualitatively change our earlier findings.

III. CONCLUSIONS

Neutrino masses and oscillations are direct evidence of physics beyond the Standard Model with potentially relevant phenomenological implications for TeV scale physics that is currently explored at the LHC. At the same time, precise measurements of lepton observables corner the parameter space of relevant models at low energies. The quality of these measurements can imply that new physics is far removed from the energy scales that the LHC or even future colliders can explore. What are the circumstances that colliders and potential discoveries at these facilities can still play a pivotal role in fingerprinting the underlying dynamics?

In this work, we have considered the type-II seesaw mechanism and its effective field theory generalization with a particular emphasis on the complementarity of low-energy coupling measurements and TeV-scale exotics. Nonminimal versions of this scenario can be described in full generality through effective field theory methods. $\mu \to 3e$ and $\mu \to e\gamma$ when understood as arising from the exchange of the type-II extended scalar sector can push the spectrum to mass scales where sensitivity is difficult to obtain. However, we show that TeV-scale modifications of the type-II scenario can readily bring down mass scales to collider-relevant scales so that future discoveries can be contextualized with low-energy neutrino phenomenology. These effects are correlated with a richer spectrum of interaction above the dynamical degrees of freedom of the type-II scenario, which again can be analyzed and constrained at the LHC and future facilities. As we exploit blind direction in the EFT-extended parameter space, it has to be admitted that the phenomenology discussed in this work is linked to fine-tuning, which we have not addressed dynamically through concrete UV completions. A possibility for the latter might be the extension of "custodial symmetry" to multiple Higgs triplets, similar to the ideas presented in, e.g., [89], which would correlate coupling modifications with the mass-eigenstates of the extended scalar spectrum (similar to how the hierarchy of charged and neutral current interaction strengths is correlated to the gauge boson masses). While we do not attempt to provide a dynamical realization of this scenario in this work, we stress that a continued search for lepton-flavor relevant new states at the LHC remains a motivated effort, even when high-precision low-energy measurements might suggest the contrary.

ACKNOWLEDGMENTS

We thank Anisha, Dave Sutherland, Graeme Crawford, Joydeep Chakrabortty, and Sabyasachi Chakraborty for helpful discussions, comments, and suggestions. C. E. is supported by the UK Science and Technology Facilities Council (STFC) under Grant No. ST/X000605/1 and the Leverhulme Trust under Grant No. RPG-2021-031. W. N. is funded by a University of Glasgow College of Science and Engineering Scholarship.

[1] T. Kajita, Nobel Lecture: Discovery of atmospheric neutrino oscillations, Rev. Mod. Phys. **88**, 030501 (2016).

[2] A. B. McDonald, Nobel Lecture: The Sudbury Neutrino Observatory: Observation of flavor change for solar neutrinos, Rev. Mod. Phys. **88**, 030502 (2016).

[3] KamLAND Collaboration, First results from KamLAND: Evidence for reactor anti-neutrino disappearance, Phys. Rev. Lett. **90**, 021802 (2003).

[4] K2K Collaboration, Indications of neutrino oscillation in a 250 km long baseline experiment, Phys. Rev. Lett. **90**, 041801 (2003).

[5] P. Minkowski, $\mu \to e\gamma$ at a rate of one out of 10^9 muon decays?, Phys. Lett. **67B**, 421 (1977).

[6] R. N. Mohapatra and G. Senjanovic, Neutrino mass and spontaneous parity nonconservation, Phys. Rev. Lett. **44**, 912 (1980).

[7] W. Konetschny and W. Kummer, Nonconservation of total lepton number with scalar bosons, Phys. Lett. **70B**, 433 (1977).

[8] M. Magg and C. Wetterich, Neutrino mass problem and gauge hierarchy, Phys. Lett. **94B**, 61 (1980).

[9] J. Schechter and J. W. F. Valle, Neutrino masses in $\mathrm{SU}(2) \times \mathrm{U}(1)$ theories, Phys. Rev. D **22**, 2227 (1980).

[10] T. P. Cheng and L.-F. Li, Neutrino masses, mixings and oscillations in $\mathrm{SU}(2) \times \mathrm{U}(1)$ models of electroweak interactions, Phys. Rev. D **22**, 2860 (1980).

[11] R. N. Mohapatra and G. Senjanovic, Neutrino masses and mixings in gauge models with spontaneous parity violation, Phys. Rev. D **23**, 165 (1981).

[12] G. Lazarides, Q. Shafi, and C. Wetterich, Proton lifetime and fermion masses in an SO(10) model, Nucl. Phys. **B181**, 287 (1981).

[13] A. Zee, Quantum numbers of Majorana neutrino masses, Nucl. Phys. **B264**, 99 (1986).

[14] K. S. Babu, Model of 'Calculable' Majorana neutrino masses, Phys. Lett. B **203**, 132 (1988).

[15] T. Han, B. Mukhopadhyaya, Z. Si, and K. Wang, Pair production of doubly-charged scalars: Neutrino mass constraints and signals at the LHC, Phys. Rev. D **76**, 075013 (2007).

[16] Anisha, U. Banerjee, J. Chakrabortty, C. Englert, M. Spannowsky, and P. Stylianou, Effective connections of $a\mu$, Higgs physics, and the collider frontier, Phys. Rev. D **105**, 016019 (2022).

[17] CMS Collaboration, A search for doubly-charged Higgs boson production in three and four lepton final states at $\sqrt{s} = 13$ TeV, Report No. CMS-PAS-HIG-16-036, CERN, 2017, https://cds.cern.ch/record/2242956.

[18] ATLAS Collaboration, Search for doubly charged Higgs boson production in multi-lepton final states with the ATLAS detector using proton–proton collisions at $\sqrt{s} = 13$ TeV, Eur. Phys. J. C **78**, 199 (2018).

[19] ATLAS Collaboration, Search for doubly charged scalar bosons decaying into same-sign W boson pairs with the ATLAS detector, Eur. Phys. J. C **79**, 58 (2019).

[20] ATLAS Collaboration, Search for doubly charged Higgs boson production in multi-lepton final states using 139 fb^{-1} of proton–proton collisions at $\sqrt{s} = 13$ TeV with the ATLAS detector, Eur. Phys. J. C **83**, 605 (2023).

[21] G. Bambhaniya, J. Chakrabortty, and S. K. Dagaonkar, Rare meson decay through off-shell doubly charged scalars, Phys. Rev. D **91**, 055020 (2015).

[22] T. Wang, Y. Jiang, Z.-H. Wang, and G.-L. Wang, Doubly-charged scalar in rare decays of the B_c meson, Phys. Rev. D **97**, 115031 (2018).

[23] J. Chakrabortty, P. Ghosh, S. Mondal, and T. Srivastava, Reconciling $(g-2)_\mu$ and charged lepton flavor violating processes through a doubly charged scalar, Phys. Rev. D **93**, 115004 (2016).

[24] R. Primulando, J. Julio, and P. Uttayarat, Scalar phenomenology in type-II seesaw model, J. High Energy Phys. 08 (2019) 024.

[25] B. Fuks, M. Nemevšek, and R. Ruiz, Doubly charged Higgs boson production at hadron colliders, Phys. Rev. D **101**, 075022 (2020).

[26] Y. Cai, T. Han, T. Li, and R. Ruiz, Lepton number violation: Seesaw models and their collider tests, Front. Phys. **6**, 40 (2018).

[27] S. Antusch, O. Fischer, A. Hammad, and C. Scherb, Low scale type II seesaw: Present constraints and prospects for displaced vertex searches, J. High Energy Phys. 02 (2019) 157.

[28] P. S. Bhupal Dev and Y. Zhang, Displaced vertex signatures of doubly charged scalars in the type-II seesaw and its left-right extensions, J. High Energy Phys. 10 (2018) 199.

[29] F. del Águila and M. Chala, LHC bounds on lepton number violation mediated by doubly and singly-charged scalars, J. High Energy Phys. 03 (**2014**) 027.

[30] CMS Collaboration, Prospects for a search for doubly charged Higgs Bosons at the HL-LHC, Report No. CMS-PAS-FTR-22-006, CERN, 2022, https://cds.cern.ch/record/2808604.

[31] D. N. Dinh, A. Ibarra, E. Molinaro, and S. T. Petcov, The $\mu - e$ conversion in nuclei, $\mu \to e\gamma, \mu \to 3e$ decays and TeV scale see-saw scenarios of neutrino mass generation, J. High Energy Phys. 08 (2012) 125.

[32] J. Chakrabortty, P. Ghosh, and W. Rodejohann, Lower limits on $\mu \to e\gamma$ from new measurements on U_{e3}, Phys. Rev. D **86**, 075020 (2012).

[33] N. D. Barrie and S. T. Petcov, Lepton flavour violation tests of type II seesaw leptogenesis, J. High Energy Phys. 01 (2023) 001.

[34] T. Li, Type II Seesaw and tau lepton at the HL-LHC, HE-LHC and FCC-hh, J. High Energy Phys. 09 (2018) 079.

[35] FCC Collaboration, FCC-ee: The lepton collider: Future circular collider conceptual design report volume 2, Eur. Phys. J. Special Topics **228**, 261 (2019).

[36] FCC Collaboration, FCC-hh: The hadron collider: Future circular collider conceptual design report volume 3, Eur. Phys. J. Special Topics **228**, 755 (2019).

[37] FCC Collaboration, FCC physics opportunities: Future circular collider conceptual design report volume 1, Eur. Phys. J. C **79**, 474 (2019).

[38] M. Williams, M. Bellis, and C. A. Meyer, Multivariate side-band subtraction using probabilistic event weights, J. Instrum. **4**, P10003 (2009).

[39] ATLAS Collaboration, Search for new phenomena in events containing a same-flavour opposite-sign dilepton pair, jets, and large missing transverse momentum in $\sqrt{s} = 13pp$ collisions with the ATLAS detector, Eur. Phys. J. C **77**, 144 (2017).

[40] ATLAS Collaboration, Higgs boson production cross-section measurements and their EFT interpretation in the

4ℓ decay channel at $\sqrt{s} = 13$ TeV with the ATLAS detector, Eur. Phys. J. C **80**, 957 (2020).
[41] ATLAS Collaboration, Measurement of the total and differential cross-sections of $t\bar{t}W$ production in pp collisions at $\sqrt{s} = 13$ TeV with the ATLAS detector, J. High Energy Phys. 05 (2024) 131.
[42] A. Alloul, N. D. Christensen, C. Degrande, C. Duhr, and B. Fuks, FeynRules 2.0—A complete toolbox for tree-level phenomenology, Comput. Phys. Commun. **185**, 2250 (2014).
[43] J. Alwall, R. Frederix, S. Frixione, V. Hirschi, F. Maltoni, O. Mattelaer, H.-S. Shao, T. Stelzer, P. Torrielli, and M. Zaro, The automated computation of tree-level and next-to-leading order differential cross sections, and their matching to parton shower simulations, J. High Energy Phys. 07 (2014) 079.
[44] C. Degrande, C. Duhr, B. Fuks, D. Grellscheid, O. Mattelaer, and T. Reiter, UFO—The Universal FeynRules Output, Comput. Phys. Commun. **183**, 1201 (2012).
[45] L. Darmé *et al.*, UFO 2.0: The 'Universal Feynman Output' format, Eur. Phys. J. C **83**, 631 (2023).
[46] M. D. Schwartz, *Anticipating the Next Discoveries in Particle Physics*, edited by R. Essig and I. Low (2018), pp. 65–100; arXiv:1709.04533.
[47] Y. Cheng, X.-G. He, F. Huang, J. Sun, and Z.-P. Xing, Electroweak precision tests for triplet scalars, Nucl. Phys. **B989**, 116118 (2023).
[48] J. Haller, A. Hoecker, R. Kogler, K. Mönig, T. Peiffer, and J. Stelzer, Update of the global electroweak fit and constraints on two-Higgs-doublet models, Eur. Phys. J. C **78**, 675 (2018).
[49] J. Fan, M. Reece, and L.-T. Wang, Possible futures of electroweak precision: ILC, FCC-ee, and CEPC, J. High Energy Phys. 09 (2015) 196.
[50] M. Gorbahn, J. M. No, and V. Sanz, Benchmarks for Higgs effective theory: Extended Higgs sectors, J. High Energy Phys. 10 (2015) 036.
[51] TLEP Design Study Working Group Collaboration, First look at the physics case of TLEP, J. High Energy Phys. 01 (2014) 164.
[52] D. M. Asner *et al.*, ILC Higgs White Paper, in Snowmass 2013: Snowmass on the Mississippi (2013), 10, arXiv:1310.0763.
[53] P. D. Bolton and S. T. Petcov, Measurements of $\mu \to 3e$ decay with polarised muons as a probe of new physics, Phys. Lett. B **833**, 137296 (2022).
[54] A. G. Akeroyd, M. Aoki, and H. Sugiyama, Lepton flavour violating decays tau—> anti-l ll and mu—> e gamma in the Higgs triplet model, Phys. Rev. D **79**, 113010 (2009).
[55] M. M. Ferreira, T. B. de Melo, S. Kovalenko, P. R. D. Pinheiro, and F. S. Queiroz, Lepton flavor violation and collider searches in a Type I + II seesaw model, Eur. Phys. J. C **79**, 955 (2019).
[56] P. F. de Salas, D. V. Forero, C. A. Ternes, M. Tortola, and J. W. F. Valle, Status of neutrino oscillations 2018: 3σ hint for normal mass ordering and improved CP sensitivity, Phys. Lett. B **782**, 633 (2018).
[57] SINDRUM Collaboration, Search for the decay $\mu^+ \to e^+e^+e^-$, Nucl. Phys. **B299**, 1 (1988).
[58] MEG Collaboration, Search for the lepton flavour violating decay $\mu^+ \to e^+\gamma$ with the full dataset of the MEG experiment, Eur. Phys. J. C **76**, 434 (2016).
[59] MEG II Collaboration, A search for $\mu^+ \to e^+\gamma$ with the first dataset of the MEG II experiment, Eur. Phys. J. C **84**, 216 (2024).
[60] B. Grzadkowski, M. Iskrzynski, M. Misiak, and J. Rosiek, Dimension-six terms in the standard model Lagrangian, J. High Energy Phys. 10 (**2010**) 085.
[61] I. Zurbano Fernandez *et al.*, High-luminosity large hadron collider (HL-LHC): Technical design report, Report No. CERN-2020-010, CERN, 2020, https://cds.cern.ch/record/2749422.
[62] V. Barger, P. Langacker, M. McCaskey, M. Ramsey-Musolf, and G. Shaughnessy, Complex singlet extension of the standard model, Phys. Rev. D **79**, 015018 (2009).
[63] G.-C. Cho, C. Idegawa, and E. Senaha, Electroweak phase transition in a complex singlet extension of the standard model with degenerate scalars, Phys. Lett. B **823**, 136787 (2021).
[64] N. Chen, T. Li, Y. Wu, and L. Bian, Complementarity of the future e^+e^- colliders and gravitational waves in the probe of complex singlet extension to the standard model, Phys. Rev. D **101**, 075047 (2020).
[65] G.-C. Cho, C. Idegawa, and R. Inumiya, A complex singlet extension of the Standard Model with a singlet fermion dark matter, arXiv:2312.05776.
[66] V. K. Oikonomou and A. Giovanakis, Electroweak phase transition in singlet extensions of the standard model with dimension-six operators, Phys. Rev. D **109**, 055044 (2024).
[67] A. Crivellin, M. Ghezzi, and M. Procura, Effective field theory with two Higgs doublets, J. High Energy Phys. 09 (2016) 160.
[68] C. Birch-Sykes, N. Darvishi, Y. Peters, and A. Pilaftsis, Accidental symmetries in the 2HDMEFT, Nucl. Phys. **B960**, 115171 (2020).
[69] Anisha, L. Biermann, C. Englert, and M. Mühlleitner, Two Higgs doublets, effective interactions and a strong first-order electroweak phase transition, J. High Energy Phys. 08 (2022) 091.
[70] Anisha, D. Azevedo, L. Biermann, C. Englert, and M. Mühlleitner, Effective 2HDM Yukawa interactions and a strong first-order electroweak phase transition, J. High Energy Phys. 02 (2024) 045.
[71] B. A. Ouazghour, A. Arhrib, K. Cheung, E.-s. Ghourmin, and L. Rahili, Charged Higgs production at the muon collider in the 2HDM, Phys. Rev. D **109**, 115009 (2024).
[72] S. Ashanujjaman, K. Ghosh, and K. Huitu, Type-II see-saw: Searching the LHC elusive low-mass triplet-like Higgses at e^-e^+ colliders, Phys. Rev. D **106**, 075028 (2022).
[73] S. Ashanujjaman and K. Ghosh, Revisiting type-II see-saw: Present limits and future prospects at LHC, J. High Energy Phys. 03 (2022) 195.
[74] R. Padhan, D. Das, M. Mitra, and A. Kumar Nayak, Probing doubly and singly charged Higgs at pp collider HE-LHC, Springer Proc. Phys. **277**, 209 (2022).
[75] J. Das and N. Kumar, Veltman criteria in the beyond standard model effective field theory of a complex scalar triplet, Phys. Rev. D **108**, 035048 (2023).

[76] Anisha, U. Banerjee, J. Chakrabortty, C. Englert, and M. Spannowsky, Extended Higgs boson sectors, effective field theory, and Higgs boson phenomenology, Phys. Rev. D **103**, 096009 (2021).
[77] U. Banerjee, J. Chakrabortty, S. Prakash, S. U. Rahaman, and M. Spannowsky, Effective operator bases for beyond standard model scenarios: An EFT compendium for discoveries, J. High Energy Phys. 01 (2021) 028.
[78] T. Hahn, Generating Feynman diagrams and amplitudes with FeynArts 3, Comput. Phys. Commun. **140**, 418 (2001).
[79] T. Hahn and M. Perez-Victoria, Automatized one loop calculations in four-dimensions and D-dimensions, Comput. Phys. Commun. **118**, 153 (1999).
[80] X. Li, D. Zhang, and S. Zhou, One-loop matching of the type-II seesaw model onto the standard model effective field theory, J. High Energy Phys. 04 (2022) 038.
[81] M. Ardu and S. Davidson, What is leading order for LFV in SMEFT?, J. High Energy Phys. 08 (2021) 002.
[82] G. Abbiendi, Status of the MUonE experiment, Phys. Scr. **97**, 054007 (2022).
[83] MUonE Collaboration, MUonE experiment at SPS, Acta Phys. Pol. B Proc. Suppl. **16**, 7 (2023).
[84] J. de Blas, Y. Du, C. Grojean, J. Gu, V. Miralles, M. E. Peskin *et al.*, Global SMEFT Fits at future colliders, in *Snowmass 2021* (2022), 6; arXiv:2206.08326.
[85] E. Celada, T. Giani, J. ter Hoeve, L. Mantani, J. Rojo, A. N. Rossia *et al.*, Mapping the SMEFT at high-energy colliders: From LEP and the (HL-)LHC to the FCC-ee, arXiv:2404.12809.
[86] A. Celis, J. Fuentes-Martin, A. Vicente, and J. Virto, DsixTools: The standard model effective field theory toolkit, Eur. Phys. J. C **77**, 405 (2017).
[87] J. Fuentes-Martin, P. Ruiz-Femenia, A. Vicente, and J. Virto, DsixTools 2.0: The effective field theory toolkit, Eur. Phys. J. C **81**, 167 (2021).
[88] J. Aebischer, J. Kumar, and D. M. Straub, Wilson: A Python package for the running and matching of Wilson coefficients above and below the electroweak scale, Eur. Phys. J. C **78**, 1026 (2018).
[89] P. S. B. Dev and A. Pilaftsis, Natural standard model alignment in the two Higgs doublet model, J. Phys. Conf. Ser. **631**, 012030 (2015).